X-692-72-395

PREPRINT

NTIS HC $4.25

NASA TM X-66106

SHOCK PHENOMENA IN INTERPLANETARY SPACE

L. F. BURLAGA

OCTOBER 1972

GSFC — GODDARD SPACE FLIGHT CENTER
GREENBELT, MARYLAND

(NASA-TM-X-66106) SHOCK PHENOMENA IN INTERPLANETARY SPACE L.F. Burlaga (NASA) Oct. 1972 45 p CSCL 03B

N73-12876

Unclas

G3/29 49146

SHOCK PHENOMENA IN INTERPLANETARY SPACE

L. F. Burlaga

Laboratory for Extraterrestrial Physics
NASA-Goddard Space Flight Center
Greenbelt, Maryland 20771

A Review presented at the Conference on Flare-Produced Shock Waves in the Corona and Interplanetary Space at the High Altitude Observatory in Boulder, Colorado 1972.

CONTENTS

I. INTRODUCTION

It is well established experimentally that the solar wind near 1 AU behaves in many respects as a compressible, supersonic, magnetogasdynamic fluid. In particular, magnetogasdynamic shock waves are observed. Some of these shocks are undoubtedly caused by flares. Others are probably not caused by flares. Ideally, this review should consider only the flare-related shocks, but this is not possible because there is as yet no unambiguous method for identifying that subset of shocks caused by solar flares.

The problem of associating shocks with flares is discussed in Section II. The observations of shock fronts and the flows behind these fronts are discussed in Section III, and synoptic views of those observations are described in the following section. Theoretical concepts and models are summarized in Section V.

Several reviews concerning interplanetary shocks have recently appeared (Hundhausen, 1972; Dryer, 1972a; Korobeinikov and Nikolayev, 1972; Burlaga, 1970; Burlaga, 1971). I refer the reader to them for details and a complete list of references. This review discusses the "big picture" with emphasis on the newest results and the key problems.

II. THE PROBLEM OF FLARE ASSOCIATION

How does one determine whether a given interplanetary shock is caused by a flare? How does one determine which flare caused a given flare-related shock? These key questions have not been answered, so one must be very cautious and critical of the flare-associations reported in the literature. This section discusses two criteria which have been used in making flare-shock associations (flare class, and type II - type IV radio bursts), and additional criteria which should be considered.

Flare Importance Class: The importance class of a flare is defined by its corrected area as seen in Hα (see Table I and Smith and Smith, 1963). It is widely believed that a shock is caused by the most "important" flare occurring a few days before the time of the shock front observation. Such a criterion is unsatisfactory for two reasons: 1) it is based on an assumption about the propagation time, which is one of the most important parameters that we would like to determine, and 2) observations show that a class 2 or 3 flare is neither a necessary nor a sufficient condition for an interplanetary shock - many class 3 flares occur which are not followed by an observable shock and conversely shocks have been observed when no class 2 or class 3 flares could be seen.

Radio Bursts: Hundhausen (1972) suggested that type II - type IV radio bursts could be used for identifying flare-related shocks and the corresponding flares. Such bursts have also been used to identify the cause of ionospheric disturbances, geomagnetic storms, and energetic solar particles (Mitra, 1970; Kundu, 1965). However, Hundhausen found that of the 22 shocks observed during the last half of 1965 and the first half of 1967, only 60% were related to II - IV radio bursts. Conversely, he found that nearly half (40%) of the II - IV bursts during the first 6 months of 1967 were not followed by interplanetary shocks. I conclude from this that II - IV radio bursts are neither a necessary nor sufficient criterion for making flare associations, although it is a step in the right direction. It is not known, however, to what extent this result depends on the completeness and sensitivity of the radio measurements. This problem merits further study.

Other Criteria: The above results indicate that we should search for other criteria for making flare-shock associations. The problem of flare associations has troubled workers in geomagnetism, aeronomy, ionospheric physics, and cosmic ray physics, so we might learn something from them. In particular, I suggest that we should consider such measurables as X-rays and U-V emissions, cm-emissions, cosmic rays and energetic particles, the total optical emission, white light (Smith and Smith, 1963) and the existence of a flash phase (Athay and Moreton, 1961). The physical causes and source positions of these emissions must be considered as well as their correlations with interplanetary observations.

III. OBSERVATIONS

I shall distinguish between two parts of a shock wave - the discontinuous shock front and the flow behind this discontinuity. These parts are sometimes loosely referred to as the "shock" and "post-shock flow", respectively.

Interplanetary shock waves are very complicated. I shall attempt to simplify their description by selecting only observations which are general characteristics of shock waves, but one must not lose sight of the complexity of real shock waves. Because we cannot unambiguously separate flare associated shock waves from other types, the following discussion concerns the general properties of all interplanetary shock waves.

Shock Fronts: Essentially, a shock front is a surface that moves relative to the ambient medium in the direction of its normal at a speed which is greater than the fast mode wave speed in that direction. Locally, the physical characteristics of the shock front depend on the shock normal and the shock "strength" (Mach number). From a global point of view, the general shape and motion of this front are of basic importance.

a. Local Shock Normals: There are now several methods for computing the shock normal at a point on the shock front (e.g. see Burlaga, 1971; Lepping and Argentiero, 1971; and Lepping, 1972) but to obtain an accurate shock normal one must choose carefully among these methods. One must be skeptical of normals which are quoted without errors, since the errors might be very large. For example, independent calculations of the normal of the July 8, 1966 shock range from 24° above the ecliptic plane to 70° below it (see Lepping 1971).

Figure 1 shows the distribution of shock normal directions for 6 typical shocks (Ogilvie and Burlaga, 1969). Similar results were found by other workers (see Hundhausen, 1972, and Bavassano et al., 1972). Note that most of the normals are close to the ecliptic plane and tend to point radially away from the sun. However, exceptional cases are sometimes observed (Hirshberg et al., 1970).

If the shocks were standing at the edges of stationary streams, they would have nearly the same shape as the streams, i.e. they would form an Archimedes spiral, and at 1 AU the normals would be $\approx 45^{\circ}$

with respect to the earth-sun line. The distributions of shock normals show quite clearly that most shocks are not corotating. This does not, however, imply that the shocks are all caused by flares.

b. Shock Strength: Perhaps the best measure of the local shock front strength is the ratio of the shock front speed (relative to the plasma) to the MHD fast-mode wave speed in the direction of the shock normal. This is the fast mode Mach number, M_f. Unfortunately, few authors compute M_f.

Since $\beta \approx 1$ near 1 AU (Burlaga and Ogilvie, 1970) $M_f \approx M_s/\sqrt{2}$ where M_s is the ordinary gasdynamic Mach number. It is generally found that $M_s \approx 3$, so $M_f \lesssim 2$. Thus, interplanetary shocks near 1 AU are intermediate strength shocks, and the simplifying assumptions of strong shock theory are not valid for them.

c. Shock Front Shape: Lepping (1971) showed that the shock normal for the July 8, 1966 event pointed $38^0 \pm 5^0$ below the ecliptic plane (Figure 2). This surprisingly large deviation from the radial direction has a simple explanation. The shock was caused by a flare high in the northern solar hemisphere (N 34^0). This flare association seems reasonably certain since the flare (2B) was accompanied by X-ray bursts, cm-wave bursts, II-IV type radio emission and energetic (> 500 MeV) protons, -Zel 'do rich et al. (1971). Thus, the observed shock normal is that which is expected if the shock surface were hemispherical with a radius of curvature of $\approx .6$ AU (Figure 2).

Ivanov (1972) found that generally shock normals are $\lesssim 40^0$ below the ecliptic if the corresponding flares are in the northern hemisphere, and vice versa, suggesting again that the radius of curvature of the shock surface is less than, but on the order of 1 AU (e.g. $\approx$.5 AU). A similar conclusion was derived from geomagnetic data (Hirshberg, 1968).

d. Shock Speeds: Local shock speeds at 1 AU range from $\approx$ 350 km/sec to $\approx$ 800 km/sec, the average being $\approx$ 500 km/sec (Hundhausen, 1972). Note that the average shock speed is only $\approx$ 25% larger than the solar wind speed ($\approx$ 400 km/sec) implying that the shocks are essentially "carried" by the solar wind.

The average shock speed between the sun and the earth is given by the transit time, T, - the time between generation by the flare and arrival at the observer. The measurements of T are controversial because of the problem of flare association. Hundhausen (1972) lists transit times ranging from $\approx$ 40 hr to $\approx$ 100 hr, the median being $\approx$ 55 hr and the corresponding mean speed being $\approx$ 600 km/sec. Akasofu and Yoshida (1967) using geomagnetic data found transit times ranging from $\approx$ 20 hr to $\approx$ 75 hr, the median being $\approx$ 40 hr with a corresponding mean speed of $\approx$ 800 km/sec. Thus the local shock speed at 1 AU is typically $\approx$ 60% to 80% of the mean speed between the sun and 1 AU. Vernov et al. (1971) have suggested that shocks are decelerated to a much greater extent.

Flows Behind the Shock Fronts: There is no really comprehensive observational study of the flow behind a shock front. Rather, the fashion has been to examine the behavior of just 1 or 2 parameters for a collection of events. The following discussion is arranged accordingly.

a. Density and Speed Profiles: The basic dynamical properties of a shock wave are revealed by the density and speed profiles. There is no general flow pattern behind shocks. Two relatively simple extremes are shown in Figures 3 and 4. In Figure 3 the flow speed and density increase for many hours after the shock front. There is thus a large increase in energy flux behind the shock. By contrast, Figure 4 shows a shock front behind which the density and flow speed (and thus the energy flux) decrease monotonically. Hundhausen (1972) refers to these two types of flows on the basis of rising and falling energy flux as "R-type" and "F-type", respectively. Other designations have also been suggested.

The variety of post-shock flows is illustrated by Figure 5 which shows 8 shock fronts (dashed vertical lines) and the flows (n, v, T_p) behind the shock fronts from Explorer 43 plasma data. Close inspection reveals that every pattern is different. Each shock wave appears to be unique. Note, however, that probably not all of these shock waves were caused by flares.

Hundhausen (1972) computed the mass and energy in excess of ambient for 6 R-type and 6 F-type shock waves, on the assumption that the area of the flare ejecta was 1/4 that of a sun-centered sphere. (Table II). Note that both energy and mass are non-zero for both types. The averages are a small fraction ($\lesssim$ 10%) of the overall efflux of the mass and energy in the coronal expansion, but are comparable to the characteristic mass and energy of a flare (Montgomery et al., 1972a).

b. Temperature: Montgomery et al. (1972b) reported that the lowest solar wind electron temperatures ($\approx 5 \times 10^4$ ^{o}K, compared to the average, $(1.5 \pm .5) \times 10^5$ ^{o}K) are observed 4 to 18 hours after the passage of a shock front. Conversely, they find that 80% of the shock fronts observed between 1969 - 1971 were followed by depressions in the electron temperatures. They suggest that the proton temperatures behave similarly.

c. Helium Enhancements: Several papers have reported a high ratio of He to H densities (.15 to .3, compared to the average of $\approx$ .05) 5 to 15 hours after the passage of a shock front. Hirshberg et al. (1972) reported that 75% of the large He enhancements (He/H $\geq$ 15%) in the period June 1965 - July 1967 were associated with solar flares of class 2 or 3. The width of the He - rich region is highly variable, (0.1 to .3) AU. Its average speed at 1 AU is 550 km/sec and is $\approx$ 80% of its mean transit speed. There is no relation between the size of the enhancement and the longitude of the flare. The relation between the He enhancement and the speed profile is not yet clear, although it is very important.

Most of the present He observations are very fragmentary. There is a great need for continuous measurements of both the He and H parameters.

d. Shape of Flare Ejecta: Long ago, Newton (1943) found that the angular half width of nascent streams (Bartles, 1940) causing magnetic storms was $\lesssim 45^{o}$. Yoshida and Akasofu (1967) arrived at a similar result. It seems that few direct studies of the angular extent of fast post shock flows have been made. One attempt has been made by Lazarus et al. (1970). Such studies require at least 2 spacecraft. Hirshberg et al. (1972) found that the angular extent of He enhancements was rather broad, extending from 65°W to 42°E.

e. Magnetic Field: Rather little has been published concerning the measurements of the magnetic field configurations behind shocks. Schatten and Schatten (1972) have statistically analyzed magnetic field data for 15 flare associated shock waves. Their results, shown in Figure 6, indicate that a large increase in the azimuthal component occurs, but the increase in the radial component is relatively small, < 15%. They also note that the field was highly disordered in the enhanced-field region. Unfortunately, the authors did not consider the plasma data, or even the shock position. They suggest that the absence of an enhanced radial field might indicate that reconnection might generally occur, separating the magnetic bottle from the sun.

IV. SYNOPTIC VIEWS

Many attempts have been made to qualitatively synthesize the flare-associated shock wave observations by drawing synoptic pictures. Two different types of synposes are generally discussed - blast waves, corresponding to shocks with decreasing n and v behind the front, and driven shocks, corresponding to shock waves with n and v increasing behind the front.

Blast waves. In the initial formulation of this model, a flare was presumed to instantaneously emit a large burst of energy, but no mass, which generated a shock front that propagated from the flare site to 1 AU. Since energy is not added continually, the fluid parameters increase at the shock front and then decay monotonically to the pre-shock state. The field configurations in such a shock wave is illustrated in Figure 7, based on a mathematical model of Parker (1963). Note the spherical symmetry. Since the observations indicate that mass probably is added, this simple synoptic picture must be modified. The effect is probably the removal of the symmetry. More observations of blast waves are much needed to test and develop the synoptic picture and to compare with the theoretical models to be discussed later. Most of the observations which have been published and described above refer to driven shocks.

Driven shocks. Early synoptic pictures of driven shocks were given by Obayashi (1967), Akasofu and Yoshida (1967), and Hirshberg (1968). Here I shall discuss only the recent synoptic picture of Hundhausen (1972), shown in Figure 8.

Ahead of the shock front one sees the radial wind and spiral magnetic field. The shock front itself is an intermediate strength, MHD shock which extends over a broad region, its radius of curvature being $\gtrsim$ .5 AU. Behind the front is ambient solar wind material which has been heated and compressed by the shock front. The observations of Schatten and Schatten (1972) suggest that the field lines should be more compressed and disordered than shown in Figure 8. The helium-rich shell is presumed to represent the arrival of new material from the flare site, an accordance with a suggestion by Lazarus and Binsack (1967). It is not clear whether this He rich material is the driver gas itself or is driven by the fast plasma behind it. The results of Hirshberg et al. (1972) suggest that the He extends over a broader extent than shown in Figure 8. Figure 8 shows a tangential discontinuity separating the driven gas from the driving gas, but there is no unambiguous observation of such a discontinuity, i.e. an isolate discontinuity which clearly separates two distinct types of material and for which all of the plasma and magnetic field parameters needed to identify a tangential discontinuity (Burlaga 1971) are available. In general, the transition may be very complex with many discontinuities present. The low temperatures behind the shock, reported by Montgomery et al. (1972b) were attributed by them to the merging of field lines. Their idea is that the question mark in Figure 8 should be replaced by closed magnetic field lines, so that heat cannot be readily conducted from the sun to the bottle; the plasma consequently cools as it expands, giving the observed low temperatures.

Another synoptic view which summarizes the most recent measurements is shown in Fig. 9. This, too, should be regarded as a working model which will change when further observations become available.

V. THEORIES OF SHOCKS

Basic Physical Ideas - Parker was the first to consider interplanetary shocks mathematically. In his usual style, Parker (1963) stripped the problem of all its complications and considered analytically two limiting cases, corresponding to instantaneous and continuous input of energy. Assuming spherical symmetry, no magnetic pressure, strong shocks, negligible wind speed, and a single fluid solar wind with negligible pressure ahead of the shock, he obtained two types of shock wave profiles - blast waves and driven shocks, corresponding to F-type and R-type shock waves, respectively, for instantaneous and continuous energy input, respectively. As Parker himself has often stressed, his calculations are simply illustrative, intending to reveal the basic physics, and should not be expected to correspond in detail to the observations. Most of the work during the last 10 years has been devoted to examining the importance of the factors that Parker neglected.

Mathematical Approaches - Two mathematical methods are used to solve the relevant equations for shock waves - similarity methods (e.g. Dryer, 1972a, and Korobeinikov and Nikolayev, 1972) and numerical methods (Hundhausen, 1972). The similarity theories exploit internal symmetries of the equations to provide insight concerning the general properties of the solutions, but they are limited in their ability to account for the variety of allowed initial conditions and boundary conditions. The numerical methods, on the other hand, are not in principle restricted by the initial and boundary conditions, but have the limitation that each solution is unique. The two approaches are thus complementary and both are valuable as long as one keeps the limitations and assumptions of each in mind. In some cases, both methods can be applied and they give equivalent results (Dryer, 1972b).

Most numerical models take the inner boundary for the calculation well beyond the critical point - usually at $\approx .1$ AU, which is at the edge of the solar envelope (the region between a few $R_\odot$ and $\approx 25\ R_\odot$, see Figure 10 and Burlaga, 1972). Figure 10 shows distance on a logarithmic scale since the solar wind is not linear. Rather little is known about the behavior of shock waves in the large region between a few solar radii and 25 $R_\odot$. Thus, in their present state, the numerical models explore "what would happen if" certain assumptions about the shocks and wind at .1 AU are satisfied. The analytical models usually specify conditions at the sun, but some assumptions in these models are not valid below .1 AU.

Parametric Studies - Here I describe the recent work on the effects of the parameters that Parker neglected. A quantity which is very useful for comparing different models is the propagation time T - the time between the generation of the shock and the arrival of the shock at the observer. In general, this depends on the energy and mass of the disturbance, the solar wind temperature, density and speed profiles, the position (r,θ,ϕ) of the observer relative to the flare, the gravitational acceleration of the sun, the solar radius and rotation rate, the characteristic dimensions of the flare site, the angular extent of the emissions, etc. (Korobeinikov, 1969).

For the simplest case of a blast wave in Parker's approximation, T depends only on the position, r, of the observer and the energy, ε, of the disturbance,

$$T \propto \frac{r^{3/2}}{\sqrt{E}} \qquad (1)$$

a. Effect of Solar Wind Speed - Since the shock speed is only $\approx 25\%$ of the wind speed at 1 AU, the shock front is carried by the solar wind, and it arrives at 1 AU much faster than one would predict if the wind speed were zero. For example, a blast wave with

$E = 10^{32}$ ergs would arrive at 1 AU in 157 hrs, according to (1), for $V_W = 0$, but considering the typical solar wind speed, $V_W \approx 400$ km/sec, one finds that T = 45 hrs (Hundhausen and Gentry, 1969).

b. Effect of Injection Time - As mentioned earlier, instantaneous injection times give rise to blast waves and infinite injection times yield "driven shock" profiles. Density and speed profiles for these two limits are shown in Figure 11a and 11c, from Hundhausen and Gentry (1969). These are numerical solutions for shocks moving into a fairly realistic ambient solar wind. An intermediate case, corresponding to an injection time of $t_i = 2.1$ hrs and $E = 1.6 \times 10^{33}$ ergs is shown in Figure 11b. Unlike the limiting cases in Figure 11a and 11c the shape of this profile will change qualitatively as the shock wave moves outward, and ultimately (when $t \gg t_i$) the profile will approach that of a blast wave.

The relation between the transit time to 1 AU and the ratio, Δ, of the injection time to the transit time is shown in Figure 12 for various energy inputs. If the injection time is very small compared to the transit time ($\Delta \ll 1$), T does not change appreciably with Δ, because the shock wave appears like a blast wave. For relatively long injection times, however, T increases rapidly with Δ. The shock wave moves more slowly in this case because the energy which drives the shock is necessarily released slowly when E is fixed and Δ is relatively large.

The preceding discussion assumes just one characteristic time. It is conceivable that the shock front near the sun is generated by a process with characteristic time t_1, and that a subsequent flow is generated by another process (possibly not even in the flare site) with characteristic time $t_0 > t_1$. This stream might steepen at 1 AU, forming the observed shock, which would then not be causally related to the shock observed near the sun.

c. Effect of Magnetic Field - Again assuming spherical symmetry, Tam and Yousefian (1972) have investigated the effect of the spiral interplanetary magnetic field on the propagation of a driven shock ($t_i \to \infty$) in the average solar wind. Computed transit times for various initial shock speeds are shown in Figure 13 for the cases $B = 0$ and $B = 5\gamma$ at 1 AU. For strong shocks, the effect of the magnetic field is negligible. For weaker shocks, the effect of magnetic field on the arrival time is found to be < 10%, but it is not certain that the latter effect is real. In any case, the effect of magnetic field on driven shocks is small, presumably because the magnetic pressure $B^2/8\pi$ is much less than the streaming energy $\rho V_W^2/2$. Since $B^2/8\pi \approx nk(T_p + T_e)$ (Burlaga and Ogilvie 1969; Ness et al. 1971), this suggests that the ambient pressure, and in particular the ambient temperature profile does not appreciably affect shock waves between the sun and 1 AU. Ultimately, of course, the magnetic and thermal pressures on the dense plug shown in Figure 11c will become significant, as discussed by Formissano and Chao (1972).

Although the magnetic field does not significantly affect the development of the shock up to 1 AU, the shock does greatly alter the field configuration. The effect of a blast wave on the direction of $\underset{\sim}{B}$ has already been discussed in relation to Figure 7 (Section III). The effect on the magnitude of $\underset{\sim}{B}$ is shown in Figure 14 from

Korobeinikov and Nikolayev (1972), where ω is defined by the radial variation of V_W, $V_W = B\ r^{\omega-2}$. Relatively little is known about the effects of driven shocks on $\underset{\sim}{B}$.

d. Non-Spherically Symmetric Shocks - DeYoung and Hundhausen (1971) numerically investigated the effect of dropping the assumption of spherical symmetry of the shock front. In particular, they asked "Given a shock front confined to a narrow cone at .1 AU, how does the shape of the surface change as the shock front moves outward into the ambient solar wind?" The result of their calculations, shown in Figure 15, is that the shock surface rapidly expands and tends to become spherical at 1 AU, with a radius of curvature of $\approx$ .5 AU on the axis of symmetry at 1 AU. This behavior is the result of the narrow bottle-like shape of the shock at .1 AU: the pressure increases everywhere across the shock surface which surrounds the bottle, causing the pressure inside the bottle to increase; this, in turn, causes the bottle to expand in all directions, making the bottle more nearly spherical.

There are two effects of the geometry on the propagation time. First, a collimated shock arrives much later than a spherical shock of the same energy (Figure 16), because the shock is weakened by the transverse expansion. Second, an observer off the axis of symmetry (say 60^0) sees the shock later (10-15 hrs) than an observer on the axis simply because the radius of curvature of the shock is less than 1 AU.

Figure 16 shows the transit time as a function of energy. The transit time decreases with increasing E, as one expects, and it is longer for a slow slower wind than for a fast wind simply because the shock is carried by the solar wind.

VI. IMPORTANT PROBLEMS

Although our knowledge of flare-associated shock waves is now fairly broad, there remains much to be learned. The extensive studies of the last several years must be followed by more intensive studies. Some of the problems which I consider to be particularly important and "ripe" are the following:

1) Establish criteria for determining whether a given shock is caused by a flare, and for identifying the flare which produces a given flare-associated shock.

2) Obtain complete descriptions of as many shock waves as possible. By complete, I mean a thorough discussion of the flare and all of the interplanetary measurements which I discussed in Section III. Special attempts should be made to identify and study blast waves.

3) Theoretically, a number of idealized models remain to be explored, e.g. non-spherically symmetric, driven shocks, with solar rotation, and shocks with magnetic fields and heat conduction. The behavior of α particles behind shock fronts must be examined quantitatively. Realistic models incorporating all of the important complications have yet to be constructed and compared with observations.

4) We know very little about the behavior of shock waves on the solar envelope. A major task of solar physicists and space physicists is to bridge this chasm, the solar envelope, which separates them.

Acknowledgements

The author acknowledges fruitful discussions with Drs. Hundhausen, Hirshberg, and Kopp. Hundhausen also contributed helpful comments on the manuscript.

This review was written while the author was a visitor at the High Altitude Observatory.

References

Akasofu, S. I., and S. Yoshida, Planet. Space Sci., 15, 39, 1967.

Athay, R. G., and G. E. Moreton, Ap. J., 133, 935, 1961.

Bartles, J., Terrestrial Magnetism, 45, 339, 1940.

Bavassano, B., F. Mariane, and N. F. Ness, Pioneer 8 Observations and Interpretations of 16 Interplanetary Shock Waves Observed in 1968, preprint, 1972.

Burlaga, L., The Solar Envelope, NASA-GSFC X-692-71-400, 1971 and in Cosmic Plasmas, ed. Schindler, 1972.

Burlaga, L. F., in Solar Terrestrial Physics; Part II, 135, D. Reidel Publishing Company, Dordrecht-Holland, 1970.

Burlaga, L. F., Space Sci. Rev., 12, 600, 1971.

Burlaga, L. F., and K. W. Ogilvie, Solar Phys., 8, 422, 1969.

Burlaga, L. F., and K. W. Ogilvie, Solar Phys., 15, 61, 1970.

DeYoung, D. S., and A. J. Hundhausen, J. Geophys. Res., 76, 2245, 1971.

Dryer, M., Interplanetary Shock Waves Generated by Solar Flares, to appear in Proceedings of the IUGG, XV General Assembly, Moscow, 1972a.

Dryer, M., Comparison of Solar Flare Energy Estimates made by Analytical and Numerical Techniques, J. Geophys. Res., in press, 1972b.

Formissano, V., and J. K. Chao, The Generation of Shock Pairs in the the Solar Wind, preprint, 1972.

Hirshberg, J., Planet. Space Sci., 16, 309, 1968.

Hirshberg, J., A. Alksne, D. S. Colburn, S. J. Bame, and A. J. Hundhausen, J. Geophys. Res., 75, 1, 1970.

Hirshberg, J., S. J. Bame, and D. L. Robbins, Solar Phys., 23, 467, 1972.

Hundhausen, A. J., Coronal Expansion and Solar Wind, in press, 1972.

Hundhausen, A. J., and R. A. Gentry, J. Geophys. Res., 74, 2908, 1969.

Ivanov, K. G., Soviet Astronomy, 15, 789, 1972.

Korobeinikov, V. P., On the Application of Dimensionality Analysis to Questions of Interplanetary Gas Motion During Solar Flares, NASA-GSFC translation ST-IS-SP-HM-10839, 1969.

Korobeinikov, V. P., and Yu. M. Nikolayev, Cosmic Electrodynamics, 3, 25, 1972.

Kundu, M. R., Solar Radio Astronomy, Interscience, New York, 1965.

Lazarus, A. J., and J. H. Binsack, Observations of the Interplanetary Plasma Associated with the July 7, 1966, Flare, presented at the Proton Flare Project Working Group of COSPAR, Tenth Planing Meeting, London, July, 1967.

Lazarus, A. J., K. W. Ogilvie, and L. F. Burlaga, Solar Phys., 13, 232, 1970.

Lepping, R. P., The July 8, 1966 Interplanetary Shock Normal in the Vicinity of the Earth, NASA-GSFC, X-692-71-365, 1971.

Lepping, R. P., J. Geophys. Res., 77, 2957, 1972.

Lepping, R. P., and P. D. Argentiero, J. Geophys. Res., 76, 4349, 1971.

Mitra, A. P., in Solar-Terrestrial Physics; Part IV, p. 1, D. Reidel Publishing Co., Dordrecht-Holland, 1970.

Montgomery, M., S. J. Bame, and A. J. Hundhausen, Energy and Mass Content of High Speed Solar Wind Streams, J. Geophys. Res., in press, 1972a.

Montgomery, M. D., J. R. Asbridge, S. J. Bame, and W. C. Feldman, EOS, Trans. AGU, 53, 503, 1972b.

Ness, N. F., A. J. Hundhausen, and S. J. Bame, J. Geophys. Res., 76, 6643, 1971.

Newton, H. W., M. Not. Roy. Ast. Soc., 103, 244, 1943.

Obayshi, T., in Solar Terrestrial Physics, ed. J. W. King and W. S. Newman, Academic Press, New York, 1967.

Ogilvie, K. W., and L. F. Burlaga, Solar Phys., 8, 422, 1969.

Parker, E. N., Interplanetary Dynamical Processes, Interscience, New York, 1963.

Schatten, K. H., and J. E. Schatten, Magnetic Field Structures in Flare Associated Solar Wind Disturbances, J. Geophys. Res., in press, 1972.

Smith, H. J., and E.v.P. Smith, Solar Flares, Macmillan, New York, 1963.

Tam, G.K.W., and V. Yousefian, J. Geophys. Res., 77, 234, 1972.

Vernov, S. N., G. P. Lyubimov, and N. V. Pereslegina, Structure of the interplanetary space from observations of low energy cosmic rays in 1965-1967, in Proc. of the Sixth Winter School on Space Physics, Part I, edited by S. N. Vernov and G. E. Kocharov, Apatity, 18 March-1 April 1969. (Transl.: Israel Program for Scientific Translations, Jerusalem 1971, p. 201).

Zel'dovich, M. A., O. M. Kurizhnykh, M. O. Madeyev, and J. A. Savenko, Geomagnetism and Aeronomy, 11, 115, 1971.

FIGURES

Fig. 1. Distribution of shock normals. θ is positive above the ecliptic. ϕ is measured from the earth-sun line, in the ecliptic plane.

Fig. 2. The July 8, 1966 shock-flare position, shock normal, and geometry of the shock front.

Fig. 3. Observations of an R-type shock wave.

Fig. 4. Observations of an F-type shock wave.

Fig. 5. The variety of post-shock flows.

Fig. 6. Magnetic field distributions in post flare flows.

Fig. 7. Magnetic field directions behind a blast wave.

Fig. 8. Hundhausen's synoptic view of a driven shock wave.

Fig. 9. A synoptic view of the observations discussed in Section III.

Fig. 10. The solar envelope.

Fig. 11. Theoretical shock wave profiles. Inner boundary at .1 AU, ambient wind at 1 AU.

Fig. 12. Relation between transit time to 1 AU and Δ, the ratio of the injection time to the transit time.

Fig. 13. Effect of magnetic field on transit time.

Fig. 14. Magnetic field intensity behind blast wave fronts. The ambient solar wind speed is $V = Ar^{\omega-2}$.

Fig. 15. Development of non-spherically symmetrical shock fronts.

Fig. 16. Transit time versus energy for spherical shocks (dashed lines) and non-spherical shocks (solid curves).

TABLE I

Importance Class	Corrected Area (in millionths) (of visible solar disc)	Corrected Area (in square degrees)
1 -	<100	<2.06
1	100-250	2.06-5.15
2	250-600	5.15-12.4
3	600-1200	12.4-24.7
3 +	>1200	>24.7

TABLE II

	R - type	F - type
<M>	3.9×10^{16} gm	1.4×10^{16} gm
<W>	6.7×10^{31} erg	1.7×10^{31} erg

☆ U.S. GOVERNMENT PRINTING OFFICE: 1972—735-963/179

Hundhausen, A. J., and R. A. Gentry, J. Geophys. Res., 74, 2908, 1969.

Ivanov, K. G., Soviet Astronomy, 15, 789, 1972.

Korobeinikov, V. P., On the Application of Dimensionality Analysis to Questions of Interplanetary Gas Motion During Solar Flares, NASA-GSFC translation ST-IS-SP-HM-10839, 1969.

Korobeinikov, V. P., and Yu. M. Nikolayev, Cosmic Electrodynamics, 3, 25, 1972.

Kundu, M. R., Solar Radio Astronomy, Interscience, New York, 1965.

Lazarus, A. J., and J. H. Binsack, Observations of the Interplanetary Plasma Associated with the July 7, 1966, Flare, presented at the Proton Flare Project Working Group of COSPAR, Tenth Planing Meeting, London, July, 1967.

Lazarus, A. J., K. W. Ogilvie, and L. F. Burlaga, Solar Phys., 13, 232, 1970.

Lepping, R. P., The July 8, 1966 Interplanetary Shock Normal in the Vicinity of the Earth, NASA-GSFC, X-692-71-365, 1971.

Lepping, R. P., J. Geophys. Res., 77, 2957, 1972.

Lepping, R. P., and P. D. Argentiero, J. Geophys. Res., 76, 4349, 1971.

Mitra, A. P., in Solar-Terrestrial Physics; Part IV, p. 1, D. Reidel Publishing Co., Dordrecht-Holland, 1970.

Montgomery, M., S. J. Bame, and A. J. Hundhausen, Energy and Mass Content of High Speed Solar Wind Streams, J. Geophys. Res., in press, 1972a.

Montgomery, M. D., J. R. Asbridge, S. J. Bame, and W. C. Feldman, EOS, Trans. AGU, 53, 503, 1972b.

Ness, N. F., A. J. Hundhausen, and S. J. Bame, J. Geophys. Res., 76, 6643, 1971.

Newton, H. W., M. Not. Roy. Ast. Soc., 103, 244, 1943.

Obayshi, T., in Solar Terrestrial Physics, ed. J. W. King and W. S. Newman, Academic Press, New York, 1967.

Ogilvie, K. W., and L. F. Burlaga, Solar Phys., 8, 422, 1969.

Parker, E. N., Interplanetary Dynamical Processes, Interscience, New York, 1963.

Schatten, K. H., and J. E. Schatten, Magnetic Field Structures in Flare Associated Solar Wind Disturbances, J. Geophys. Res., in press, 1972.

Smith, H. J., and E.v.P. Smith, Solar Flares, Macmillan, New York, 1963.

Tam, G.K.W., and V. Yovsefian, J. Geophys. Res., 77, 234, 1972.

Vernov, S. N., G. P. Lyubimov, and N. V. Pereslegina, Structure of the interplanetary space from observations of low energy cosmic rays in 1965-1967, in Proc. of the Sixth Winter School on Space Physics, Part I, edited by S. N. Vernov and G. E. Kocharov, Apatity, 18 March-1 April 1969. (Transl.: Israel Program for Scientific Translations, Jerusalem 1971, p. 201).

Zel'dovich, M. A., O. M. Kurizhnykh, M. O. Madeyev, and J. A. Savenko, Geomagnetism and Aeronomy, 11, 115, 1971.

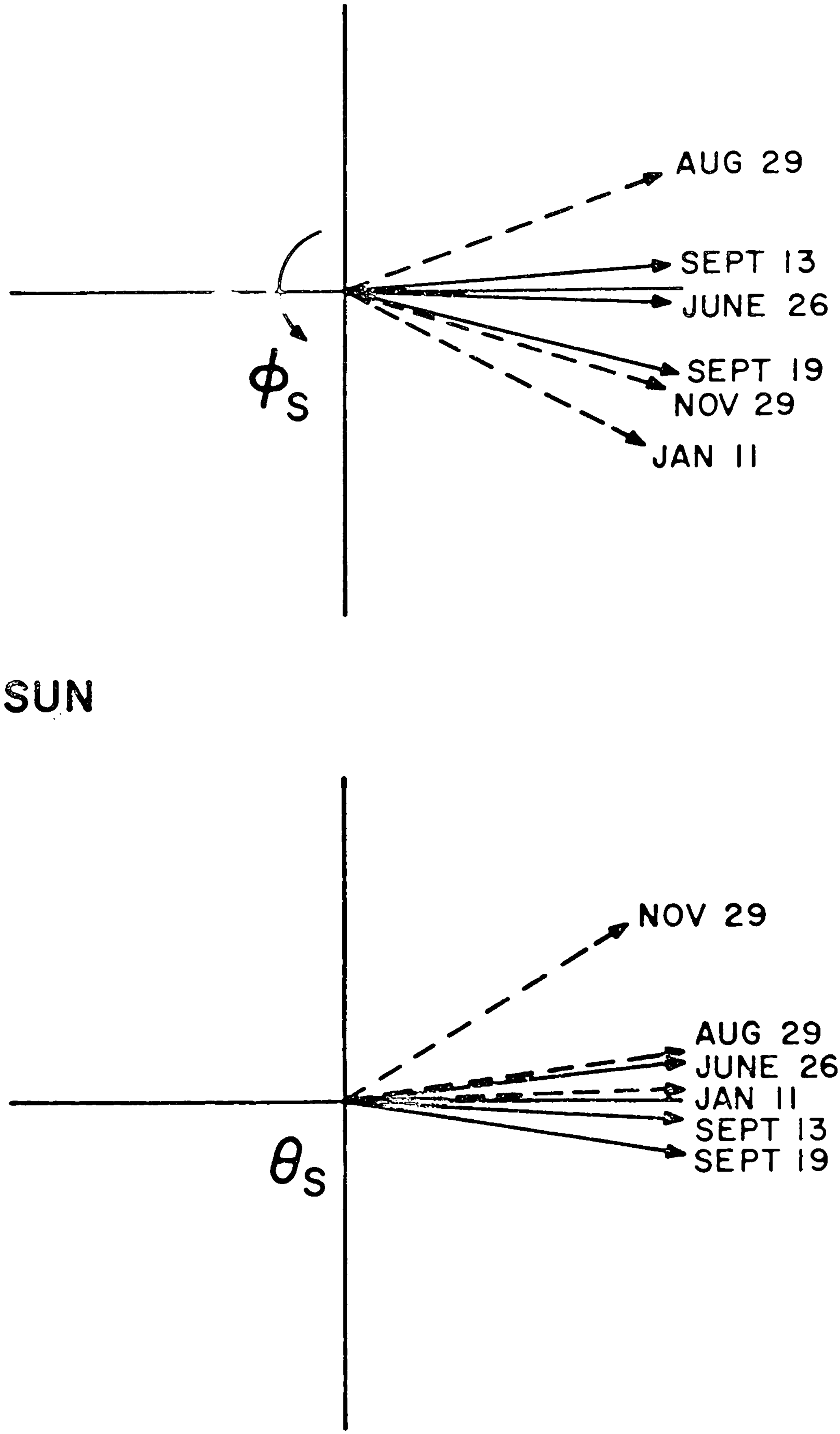
AUG 29
SEPT 13
JUNE 26
SEPT 19
NOV 29
JAN 11
ϕ_S
SUN
NOV 29
AUG 29
JUNE 26
JAN 11
SEPT 13
SEPT 19
θ_S

FIGURE 1

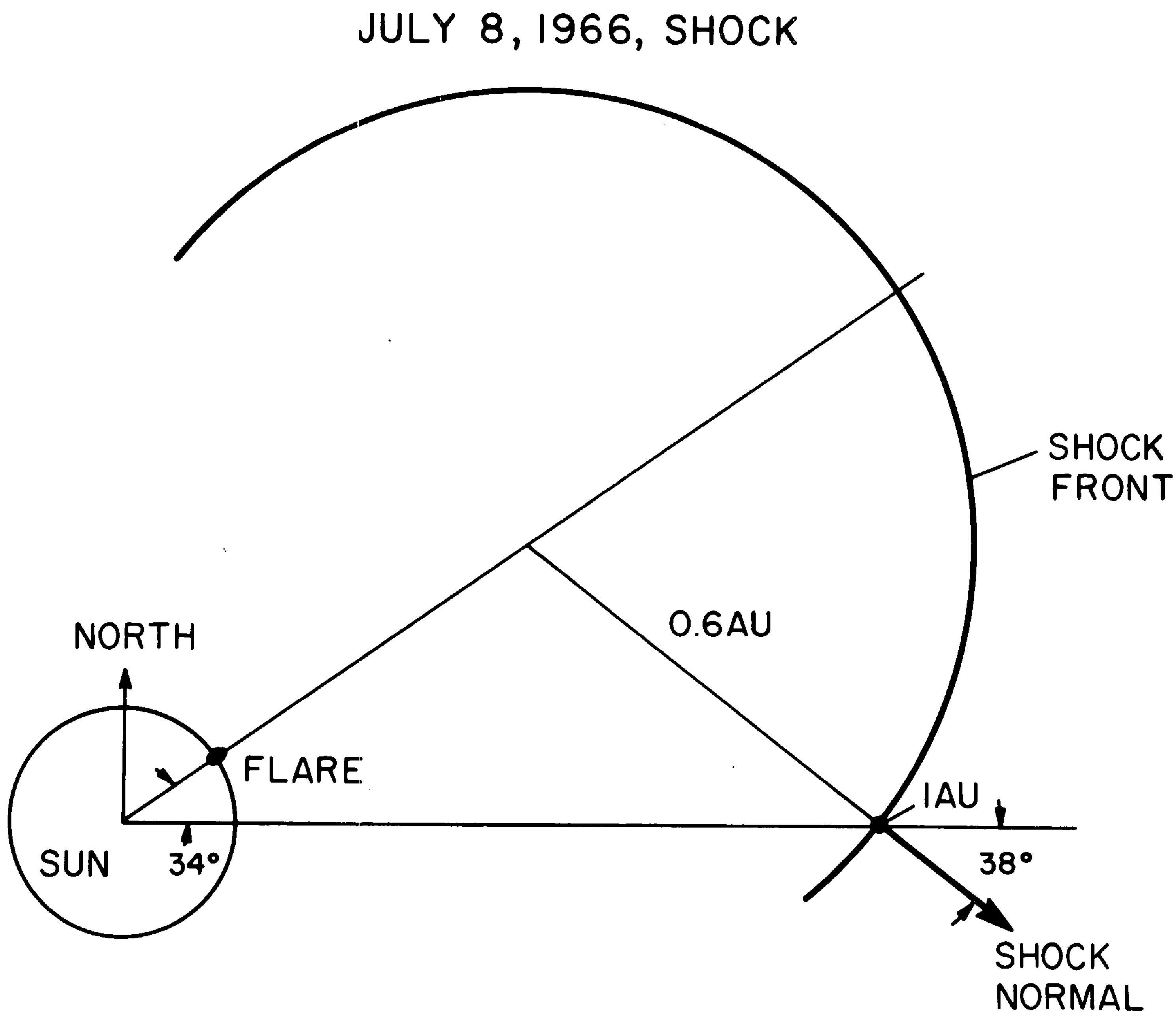
JULY 8, 1966, SHOCK
SHOCK
FRONT
NORTH
0.6AU
FLARE
1AU
SUN
34°
38°
SHOCK
NORMAL

FIGURE 2

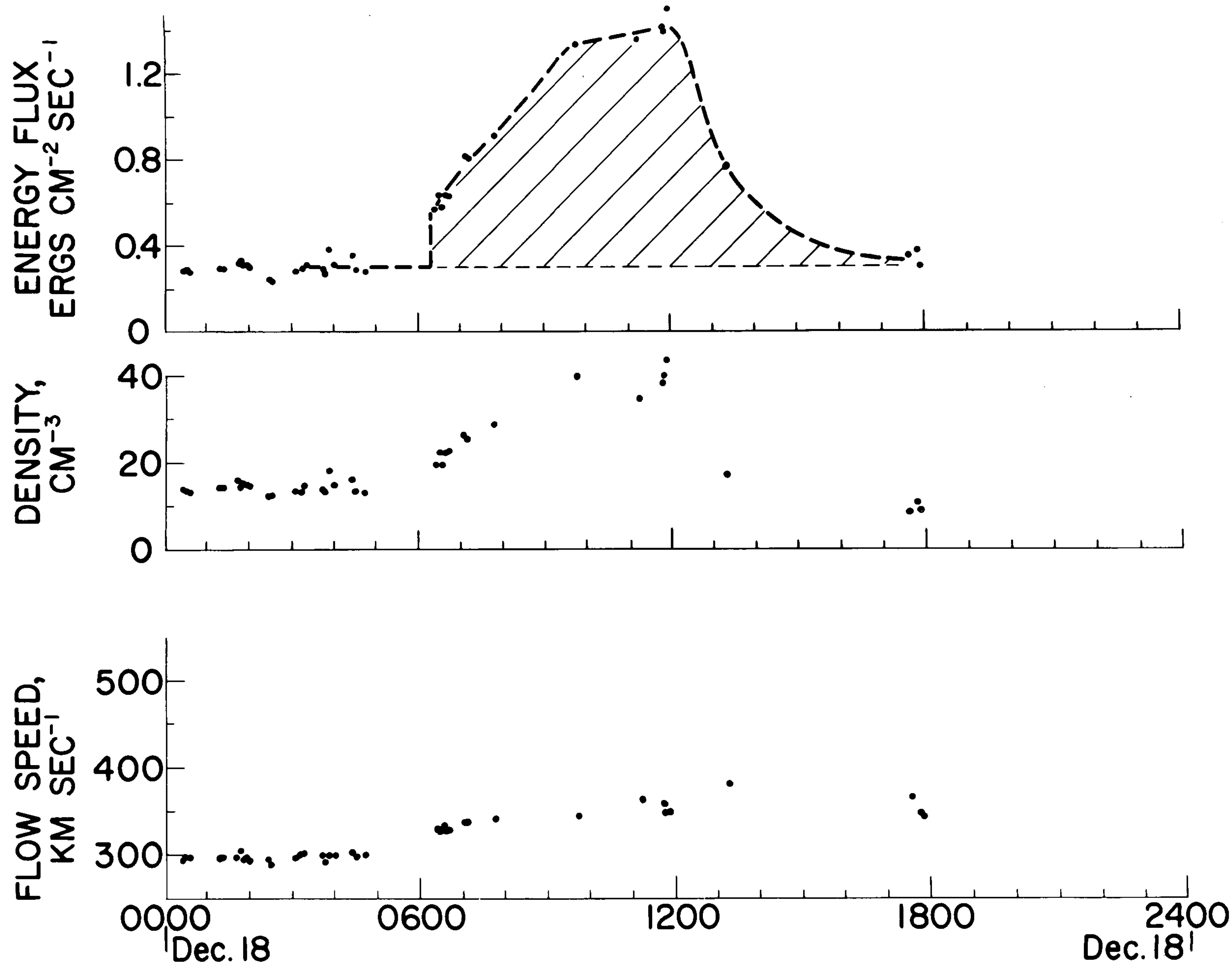

ENERGY FLUX
ERGS CM-2 SEC-1
1.2
0.8
0.4
0
DENSITY,
CM-3
40
20
0
FLOW SPEED,
KM SEC-1
500
400
300
0000
Dec. 18
0600
1200
1800
2400
Dec. 18

FIGURE 3

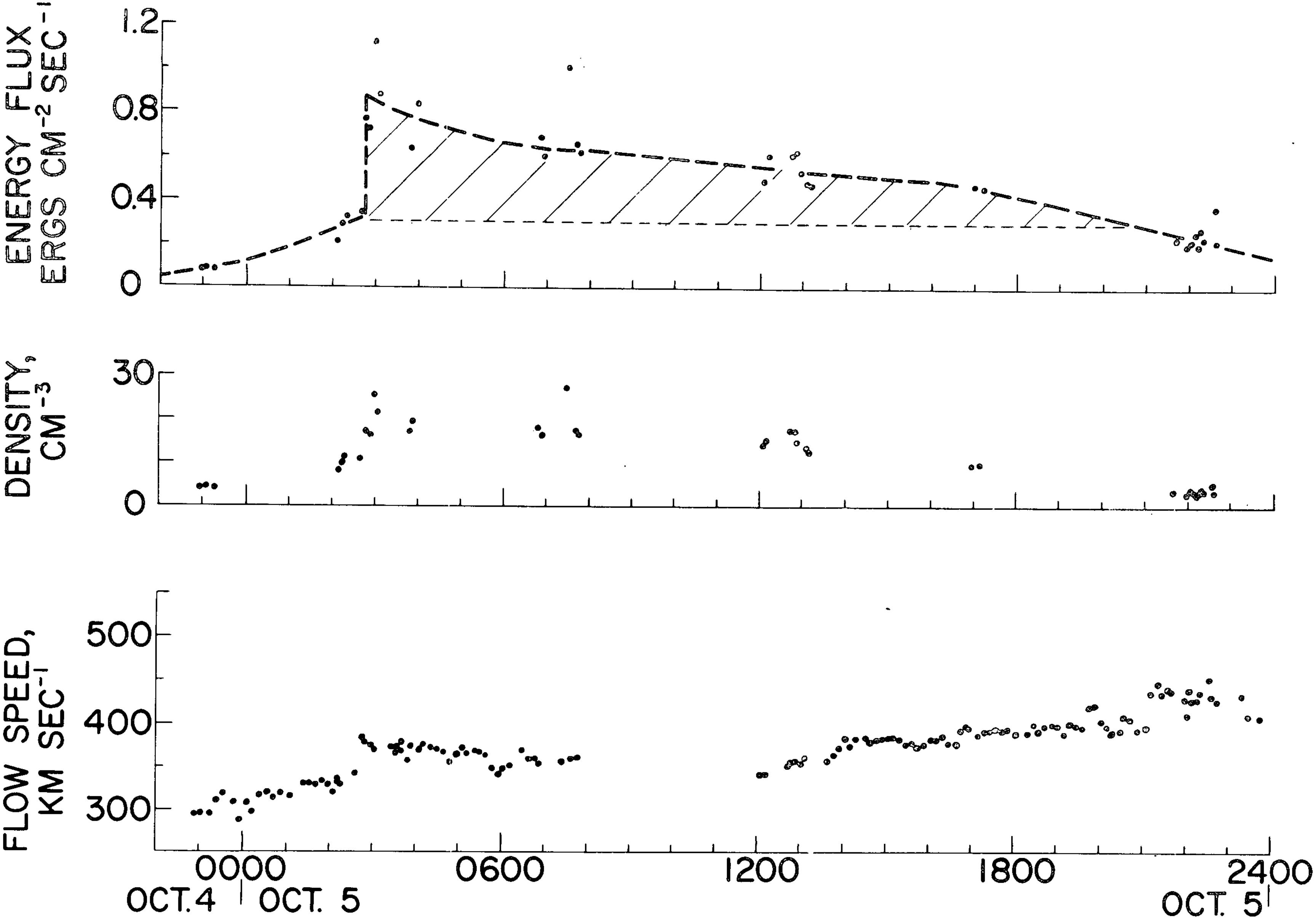
ENERGY FLUX
ERGS CM^{-2} SEC^{-1}
1.2
0.8
0.4
0
DENSITY,
CM^{-3}
30
0
FLOW SPEED,
KM SEC^{-1}
500
400
300
0000
0600
1200
1800
2400
OCT.4
OCT. 5
OCT. 5

FIGURE 4

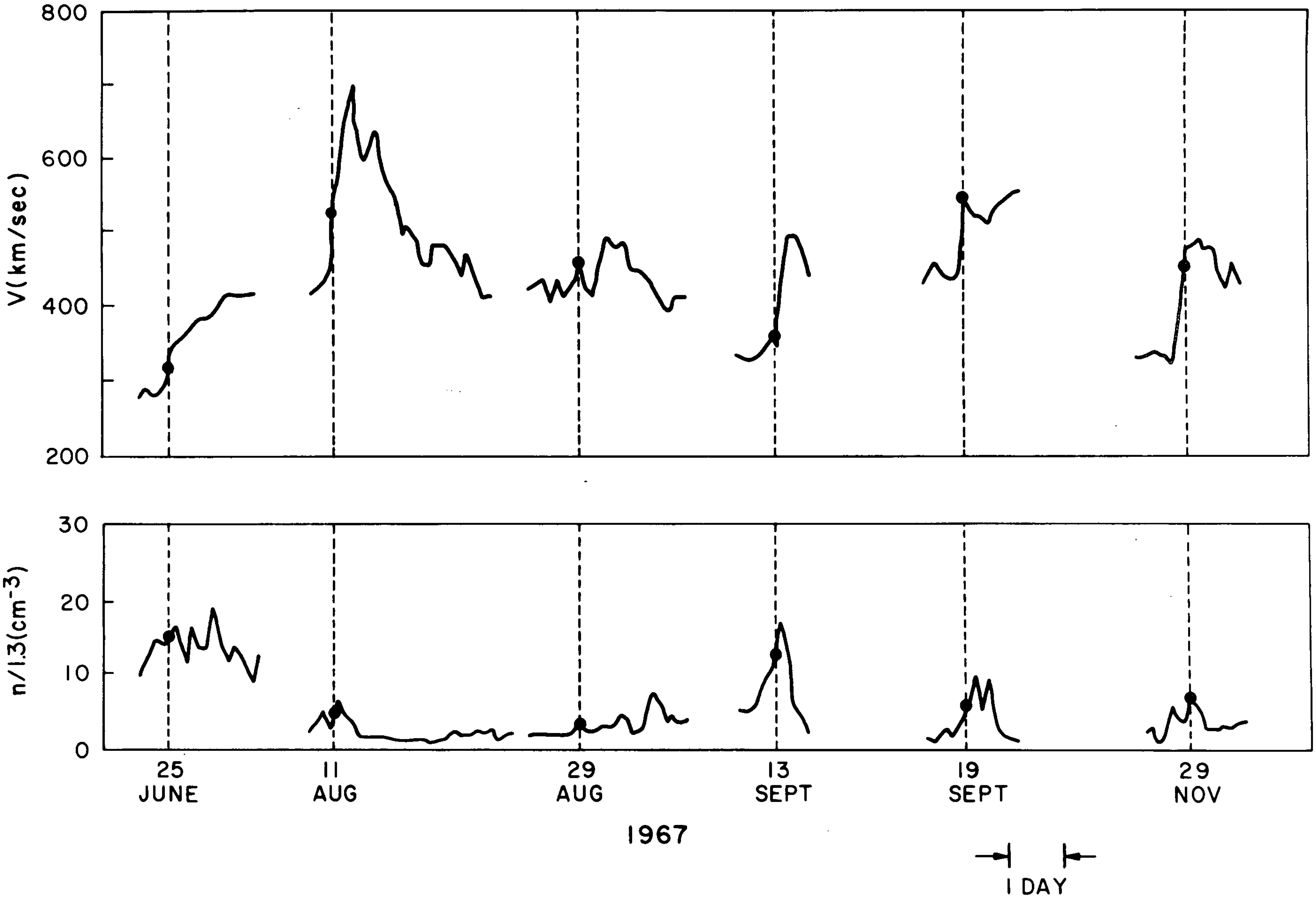
800
600
400
200
V(km/sec)
30
20
10
0
n/1.3(cm^-3)
25
JUNE
11
AUG
29
AUG
13
SEPT
19
SEPT
29
NOV
1967
1 DAY

FIGURE 5

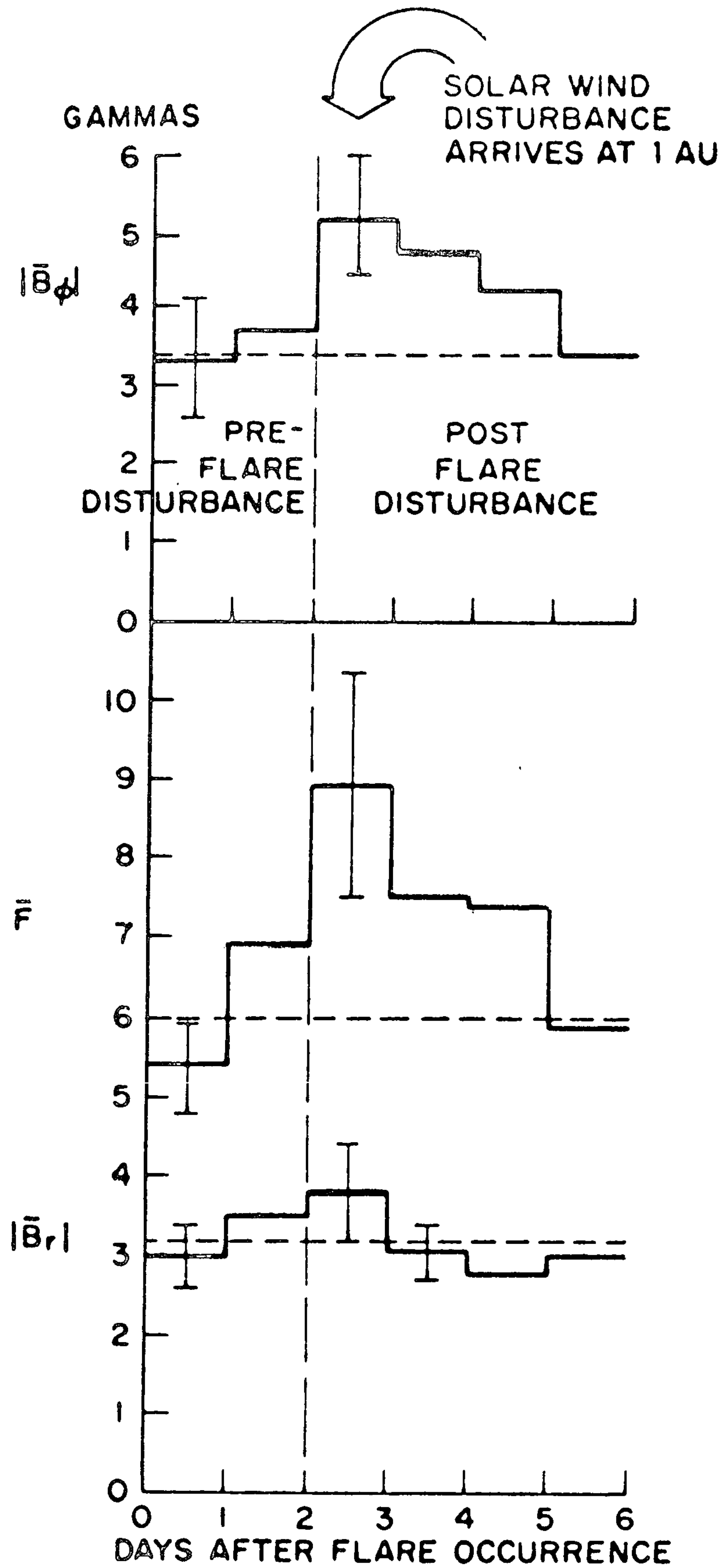
SOLAR WIND
DISTURBANCE
ARRIVES AT 1 AU
GAMMAS
6
5
4
3
2
1
0
$|\bar{B}_\phi|$
PRE-
FLARE
DISTURBANCE
POST
FLARE
DISTURBANCE
10
9
8
7
6
5
4
3
2
1
0
$\bar{F}$
$|\bar{B}_r|$
0
1
2
3
4
5
6
DAYS AFTER FLARE OCCURRENCE

FIGURE 6

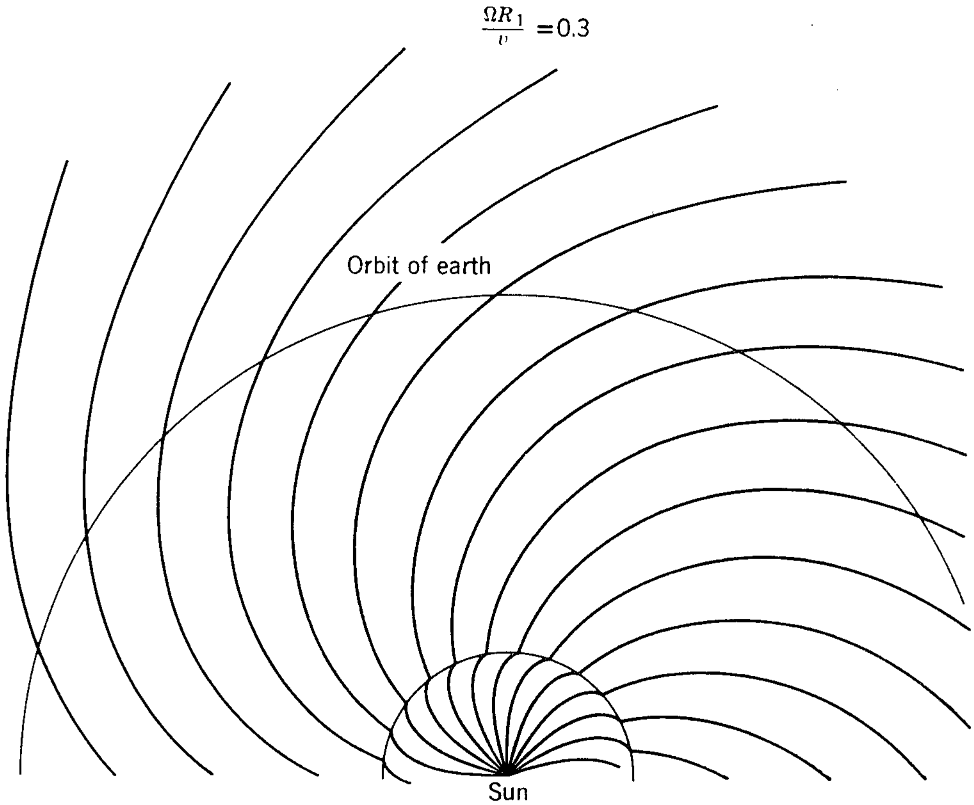

$\frac{\Omega R_1}{v} = 0.3$
Orbit of earth
Sun

(*a*)

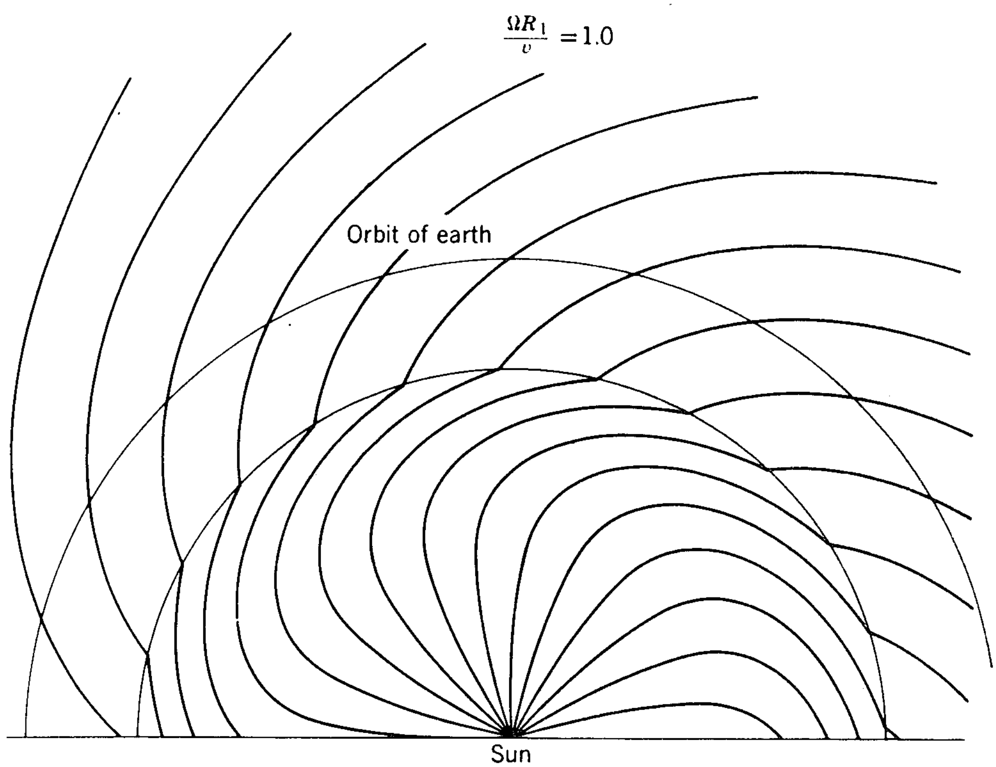

$\frac{\Omega R_1}{v} = 1.0$
Orbit of earth
Sun

(*b*)

FIGURE 7

POSSIBLE GEOMETRY OF A FLARE - PRODUCED SHOCK WAVE, SYNTHESIZED FROM OBSERVATIONS

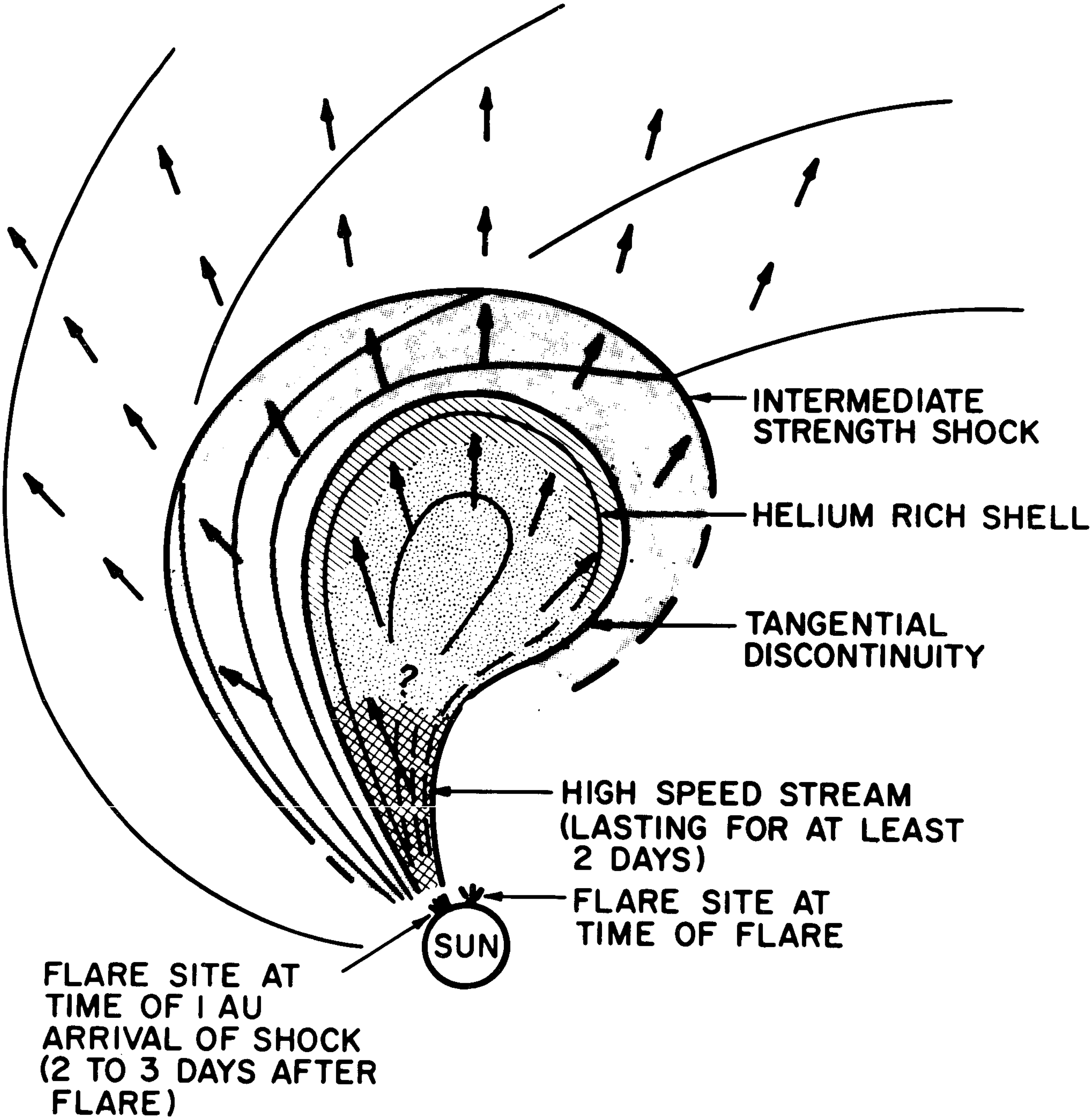

FIGURE 8

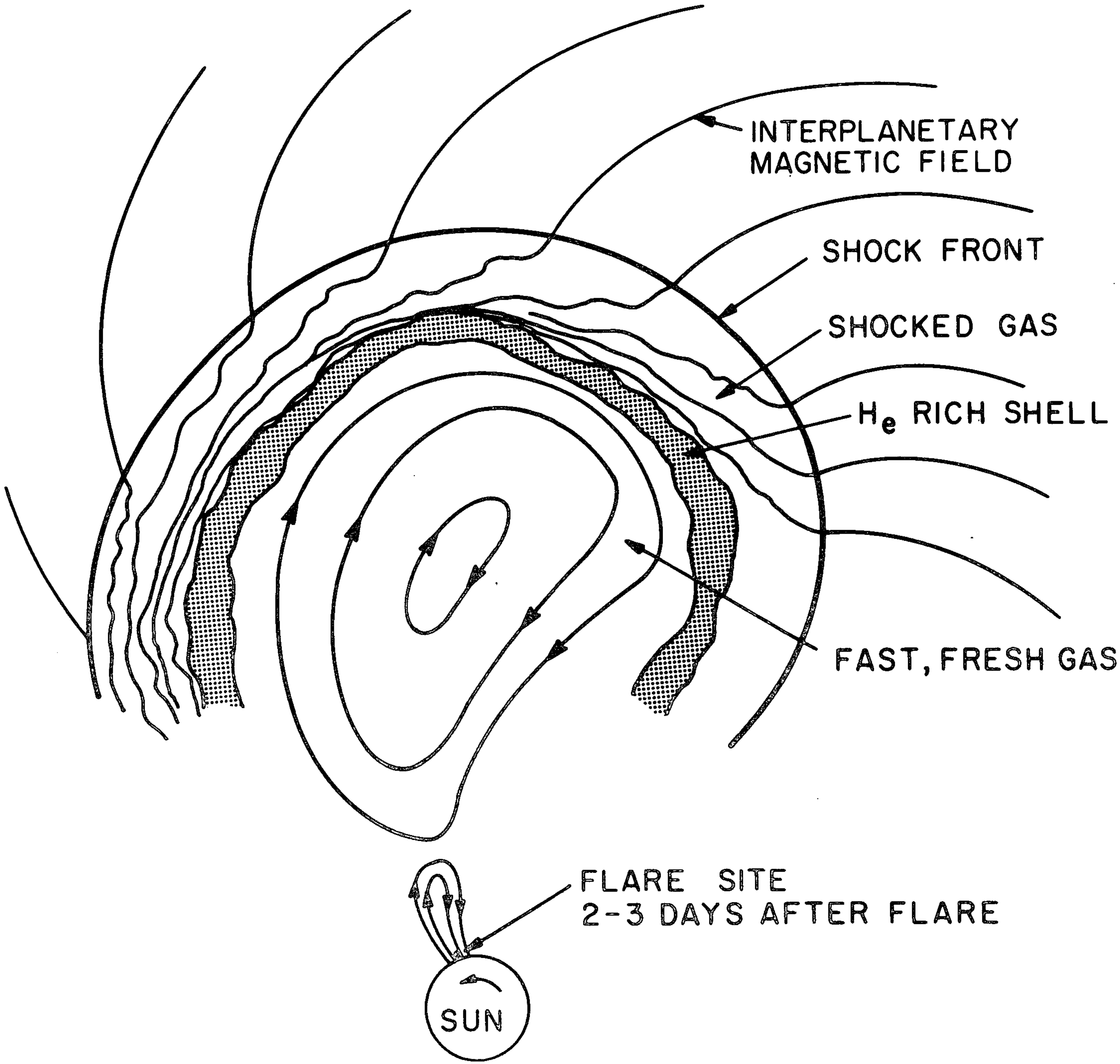
INTERPLANETARY
MAGNETIC FIELD
SHOCK FRONT
SHOCKED GAS
H_e RICH SHELL
FAST, FRESH GAS
FLARE SITE
2-3 DAYS AFTER FLARE
SUN

FIGURE 9

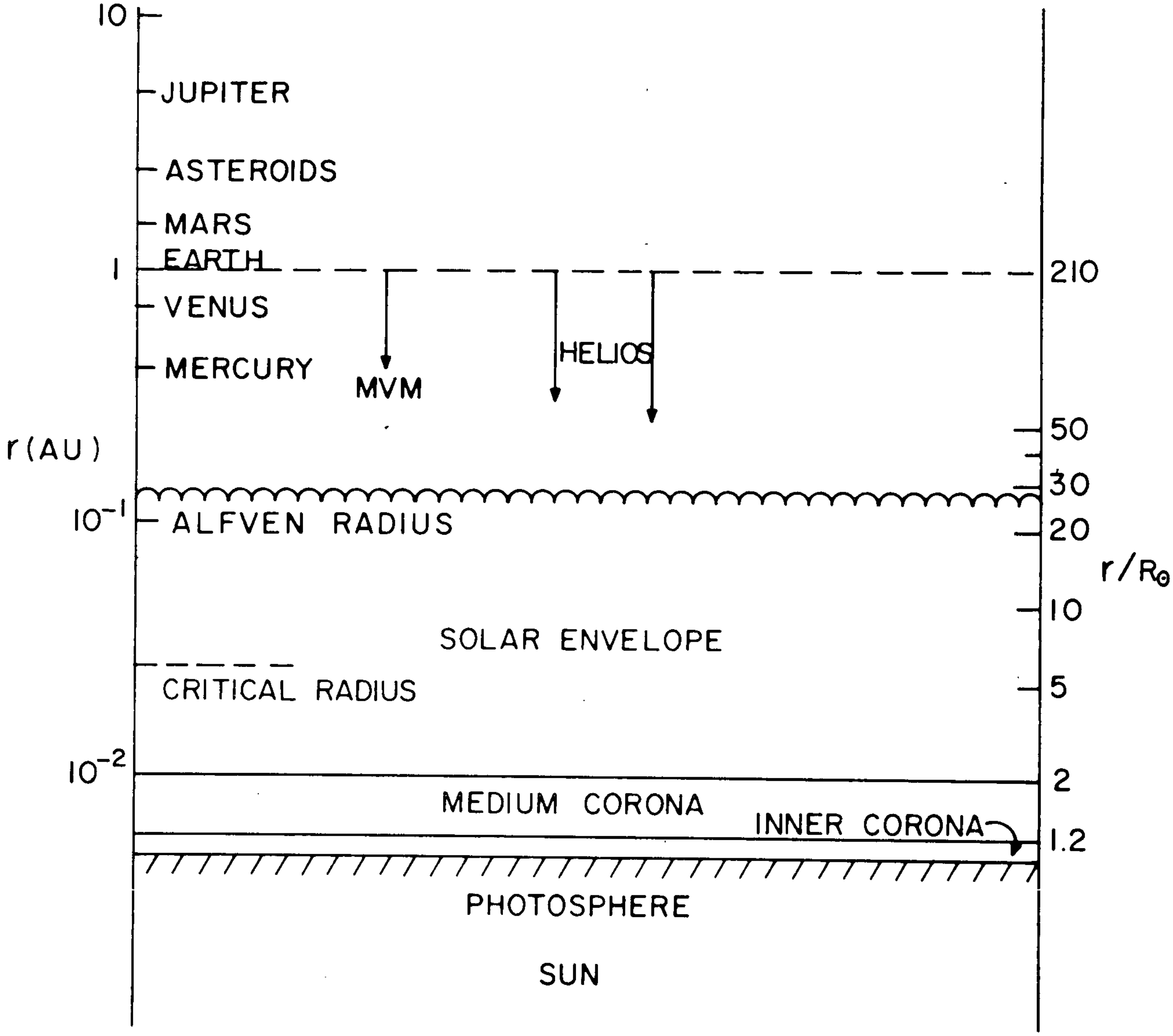

10
JUPITER
ASTEROIDS
MARS
EARTH
1
VENUS
MERCURY
MVM
HELIOS
r (AU)
10^{-1}
ALFVEN RADIUS
SOLAR ENVELOPE
CRITICAL RADIUS
10^{-2}
MEDIUM CORONA
INNER CORONA
PHOTOSPHERE
SUN
210
50
30
20
$r/R_\odot$
10
5
2
1.2

FIGURE 10

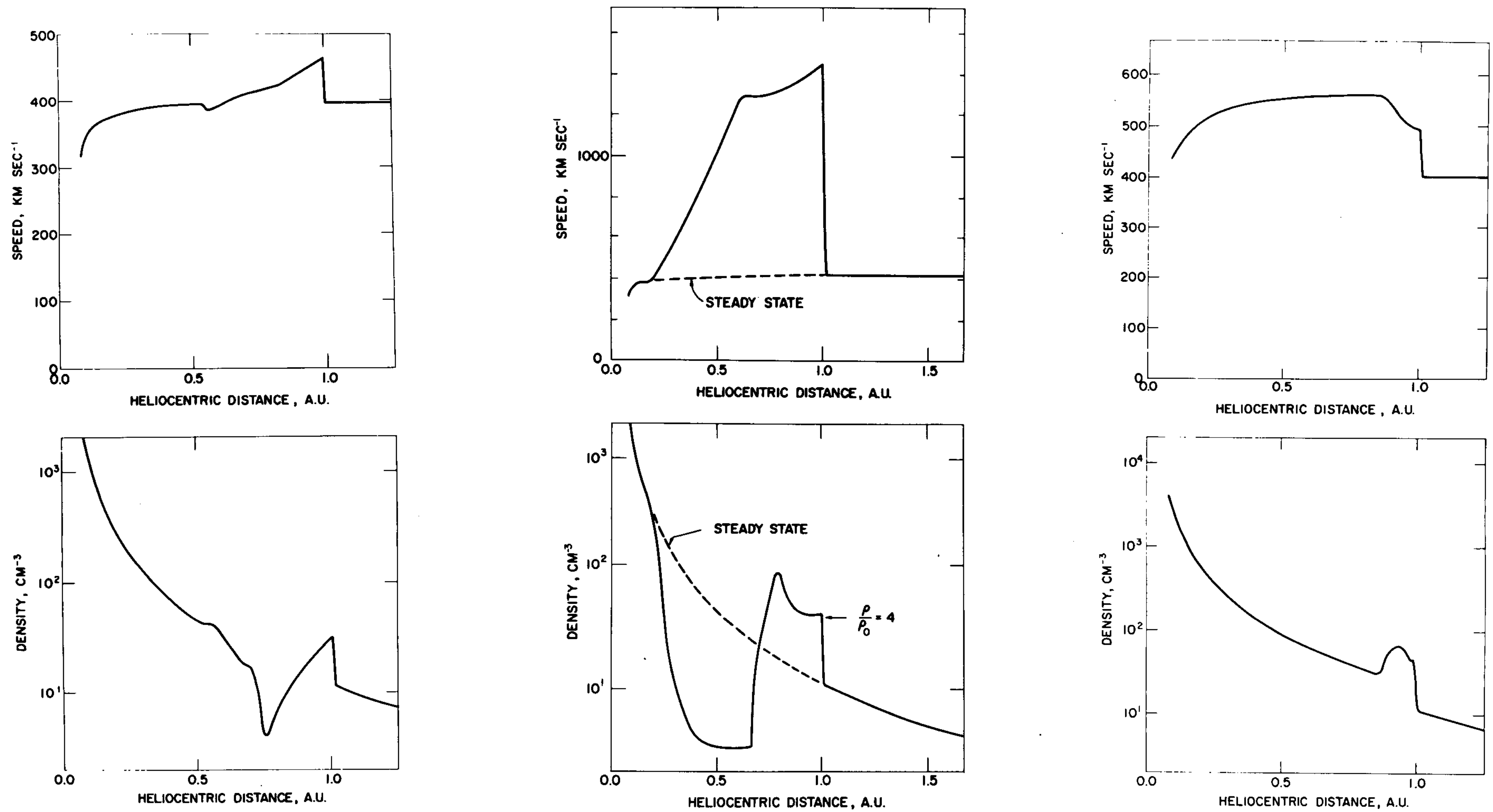
SPEED, KM SEC⁻¹
DENSITY, CM⁻³
HELIOCENTRIC DISTANCE, A.U.
STEADY STATE
$\frac{\rho}{\rho_0} = 4$

FIGURE 11

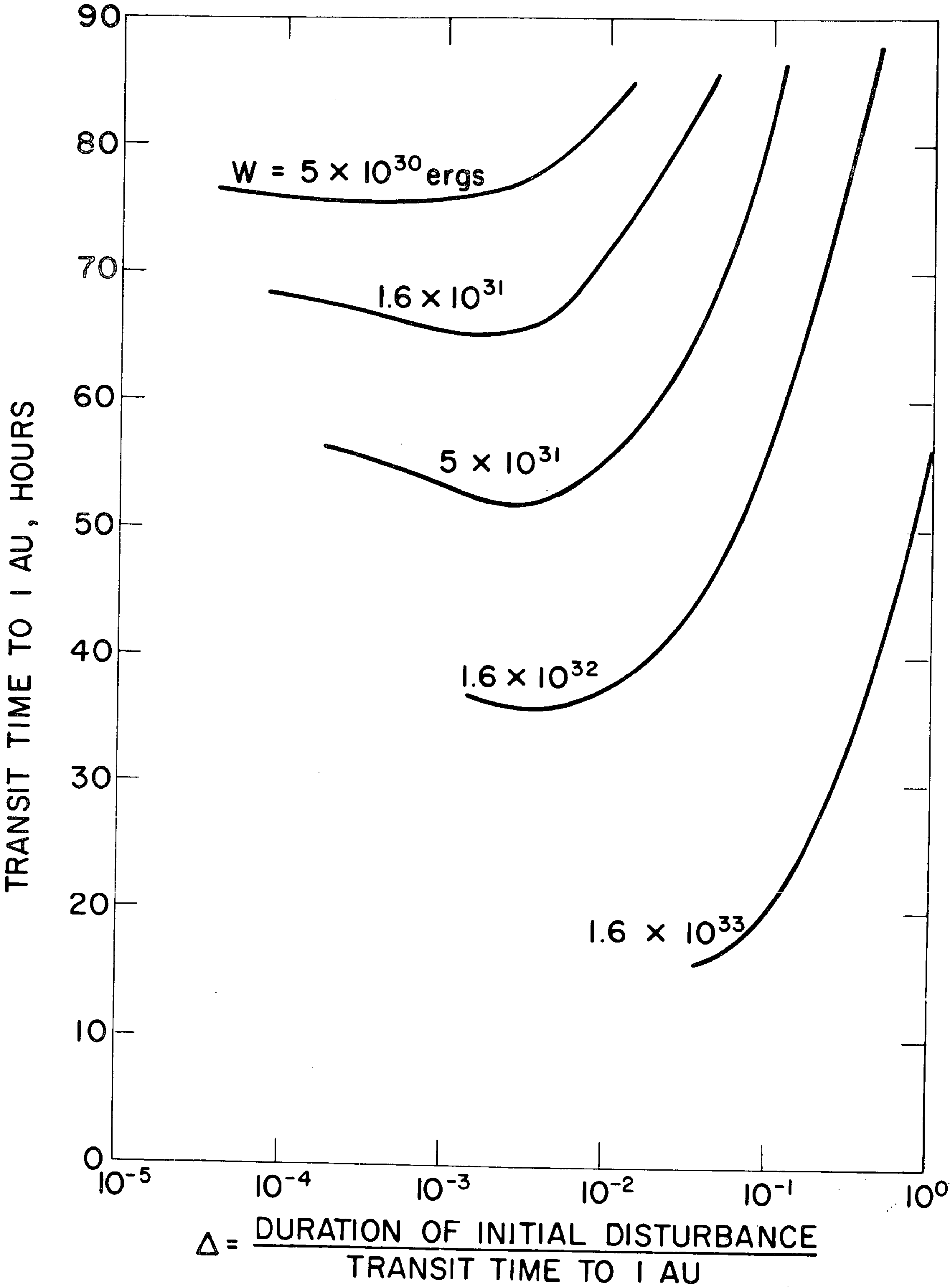

90
80
70
60
50
40
30
20
10
0
TRANSIT TIME TO 1 AU, HOURS
W = 5 × 10^30 ergs
1.6 × 10^31
5 × 10^31
1.6 × 10^32
1.6 × 10^33
10^-5
10^-4
10^-3
10^-2
10^-1
10^0
Δ = DURATION OF INITIAL DISTURBANCE / TRANSIT TIME TO 1 AU

FIGURE 12

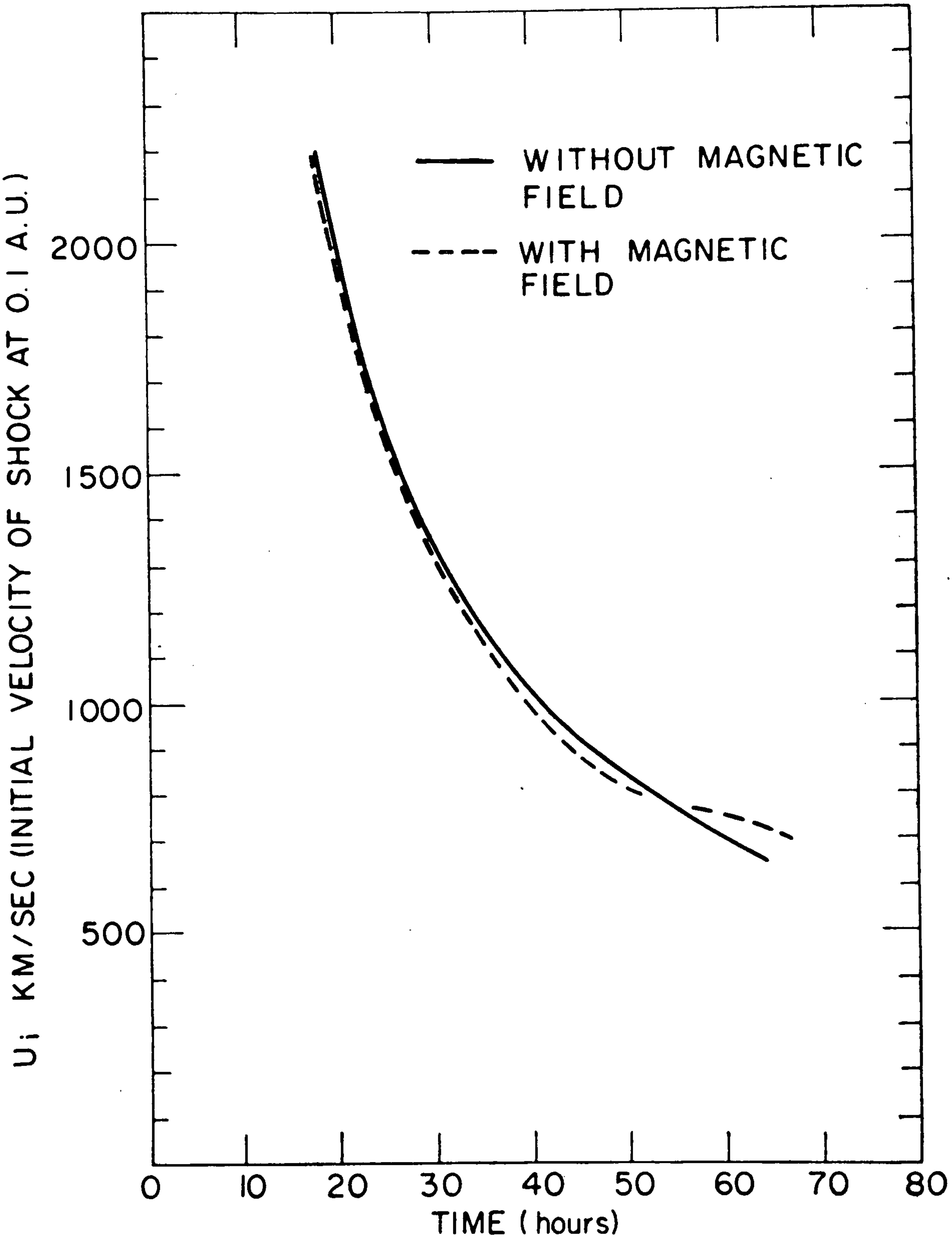

Arrival time at 1 AU for shocks with various initial speeds.

FIGURE 13

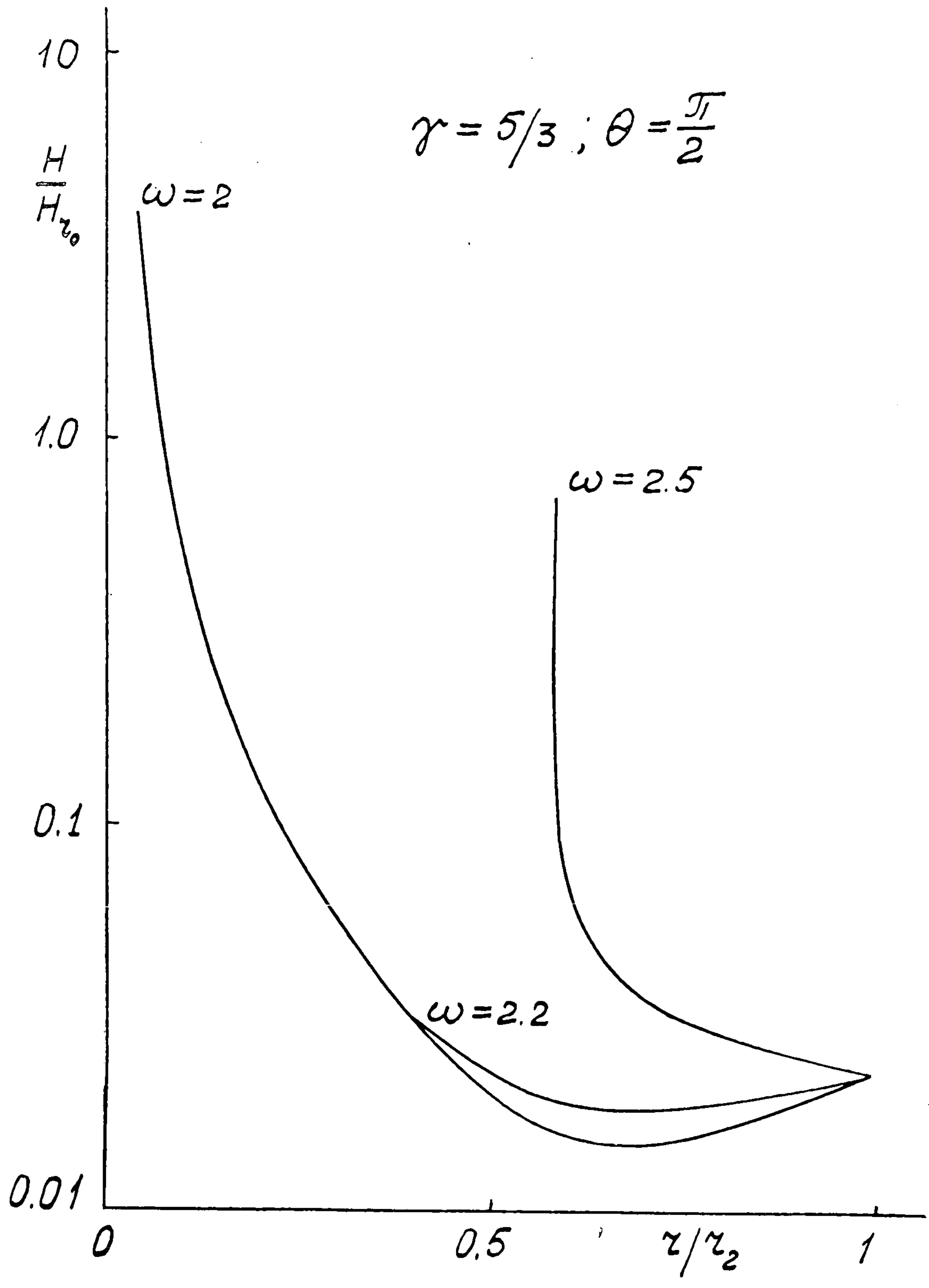

Magnetic field distribution in the blast wave model.

FIGURE 14

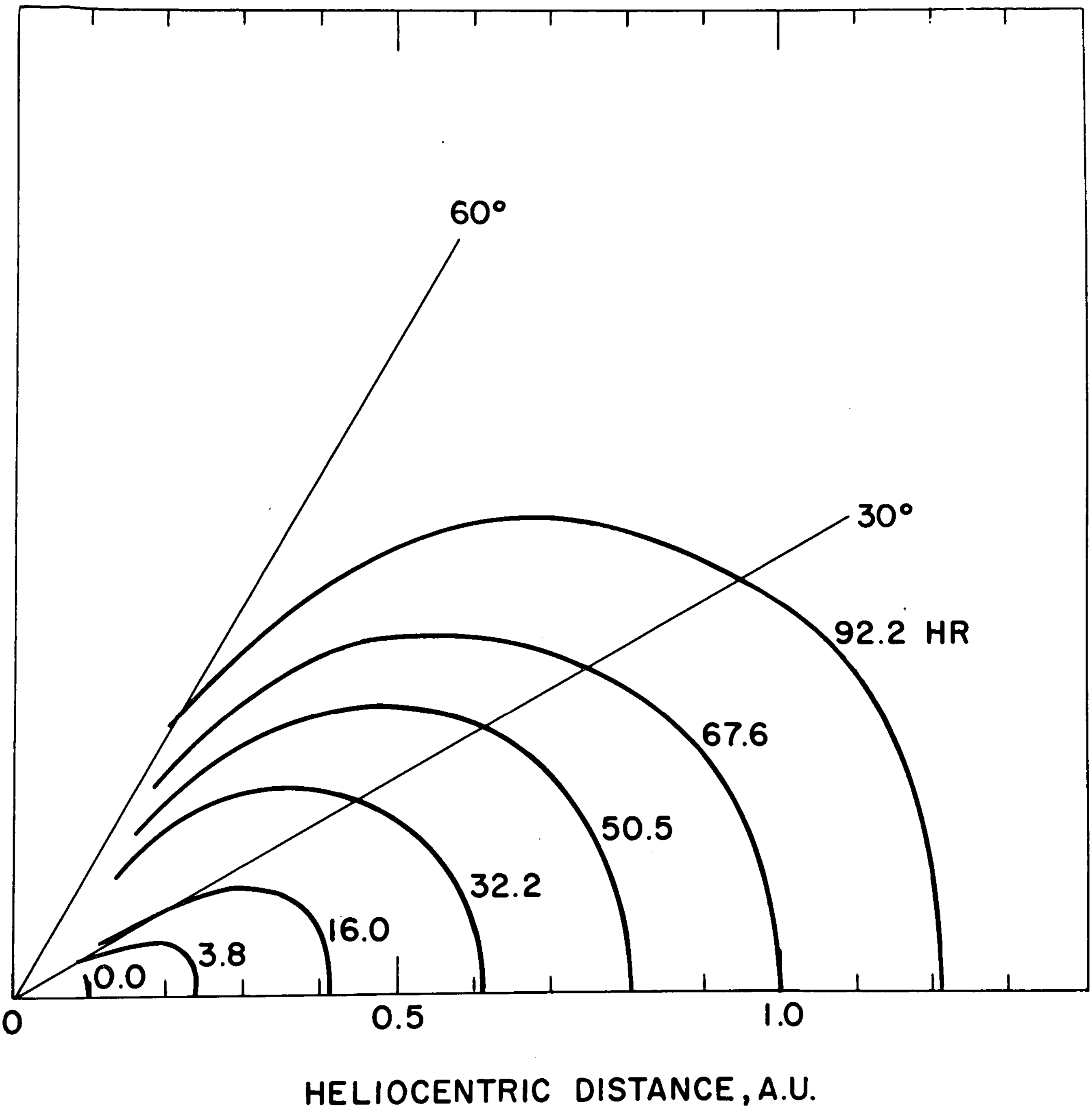

60°
30°
92.2 HR
67.6
50.5
32.2
16.0
3.8
0.0
0
0.5
1.0
HELIOCENTRIC DISTANCE, A.U.

FIGURE 15

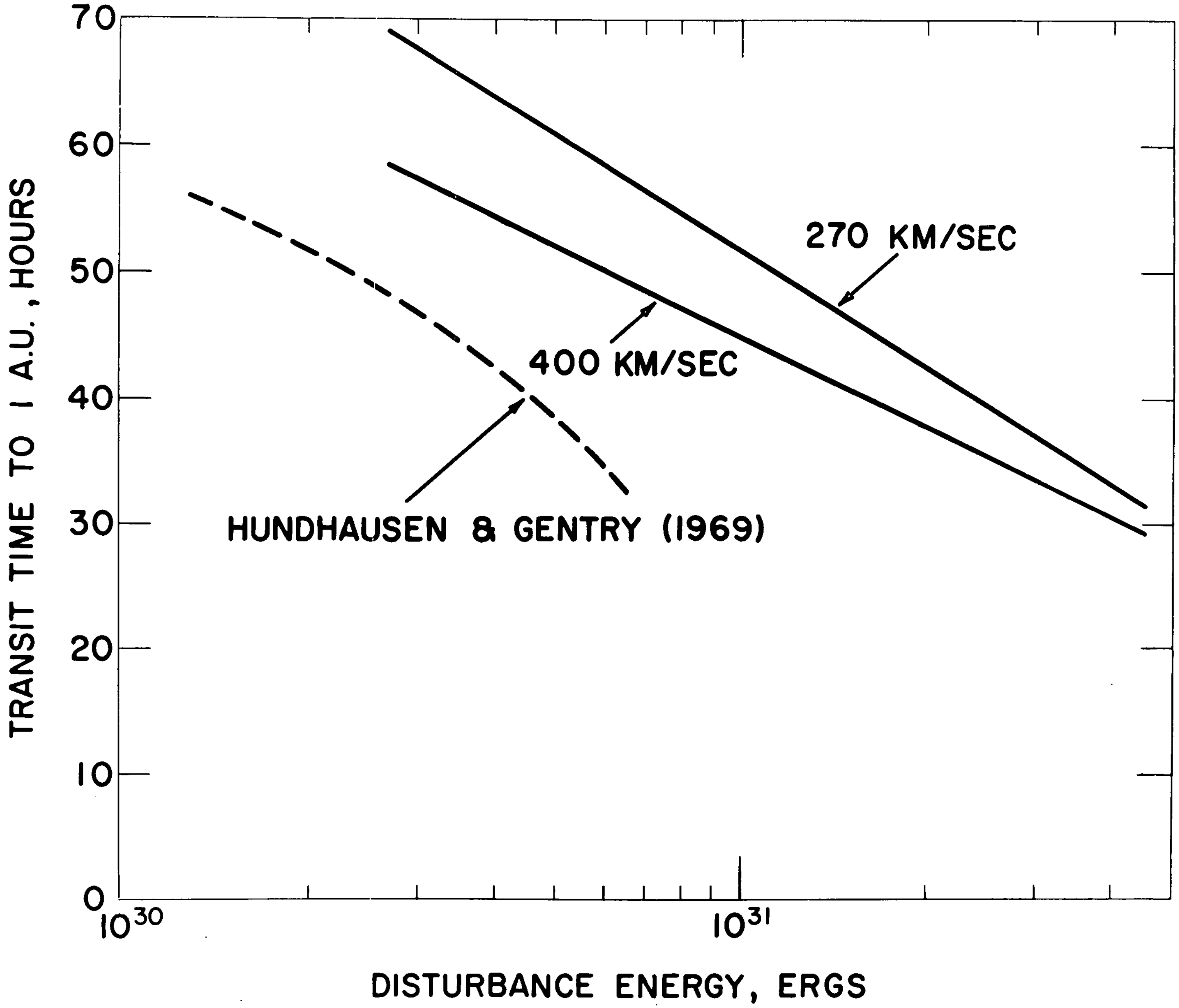
70
60
50
40
30
20
10
0
TRANSIT TIME TO 1 A.U., HOURS
270 KM/SEC
400 KM/SEC
HUNDHAUSEN & GENTRY (1969)
10^30
10^31
DISTURBANCE ENERGY, ERGS

FIGURE 16